Ultrafast Coherent Dynamics of a Photonic Crystal All-Optical Switch

Pierre Colman
DTU Fotonik, Technical University of Denmark, DK-2800 Kongens Lyngby, Denmark
and IEF Institut d'Electronique Fondamentale, Université Paris-Sud, F 91405 Orsay, France

Per Lunnemann, Yi Yu, and Jesper Mørk*
DTU Fotonik, Technical University of Denmark, DK-2800 Kongens Lyngby, Denmark
(Received 21 April 2016; published 29 November 2016)

We present pump-probe measurements of an all-optical photonic crystal switch based on a nanocavity, resolving fast coherent temporal dynamics. The measurements demonstrate the importance of coherent effects typically neglected when considering nanocavity dynamics. In particular, we report the observation of an idler pulse and more than 10 dB parametric gain. The measurements are in good agreement with a theoretical model that ascribes the observation to oscillations of the free-carrier population in the nanocavity. The effect opens perspectives for the realization of new all-optical photonic crystal switches with unprecedented switching contrast.

DOI: 10.1103/PhysRevLett.117.233901

Over the past decade, there has been significant progress in integrated optics in terms of decreasing both footprint and energy consumption. The control of light with light, such as active switching operations, would enable enhanced functionality, but the energy consumption devoted to each individual function must be of the order of a few fJ/bit [1]. Planar photonic crystal (PhC) cavities are promising candidates for the realization of all-optical switching operations thanks to their small volume, high quality factor, integrability [2–7], and low switching energy [7].

Classical schemes for all-optical switching using a PhC cavity involve the dynamical control of the cavity resonance via a pump pulse [2,8,9], which shifts the cavity's resonance, thus controlling the transmission of a subsequent probe [see Fig. 1(b)]. The cavity resonance can be changed either by the Kerr effect [10] or through the dispersion caused by free carriers (FCD) [11] generated by the absorption of the pump. The latter process is usually preferred, as it builds up over time and therefore requires less pump power.

The switching energy can be further minimized by taking advantage of a combination of linear absorption and nonlinear two-photon absorption (TPA) [7,12] in a configuration that benefits from the band filling dispersion [13]. Even lower switching energy can be obtained by using quantum dots as an absorptive material instead of bulk material: They exhibit extreme nonlinearity and absorption saturation properties and can be operated in the few-photon regime [14,15]. However, these configurations require complex material engineering and showed limitations in terms of switching speed due to a long free-carrier lifetime. In particular, a long carrier lifetime gives rise to strong patterning effects when operated at a high data rate [5,16].

The use of a small cavity with a high-Q factor and short pulses favors the use of TPA-based carrier generation [17]. Further reduction of the switching energy may be obtained using waveguide-cavity designs exhibiting Fano resonances [18–20], where a nonlinear regeneration mechanism has been shown to improve the response [21].

Despite a good understanding of the dynamics of PhC switches on the long time scale [5,22,23], the switching dynamics on short time scales as well as the possible role of coherent effects have so far received little attention. In addition to the resonance shift, caused by the FCD, the PhC cavity is also known to induce, during the first stage of its nonlinear evolution, an adiabatic frequency shift of the light [24–27] caused by temporal changes of its refractive index that can also result in other coherent effects. The impact of these effects on the switching dynamics has not

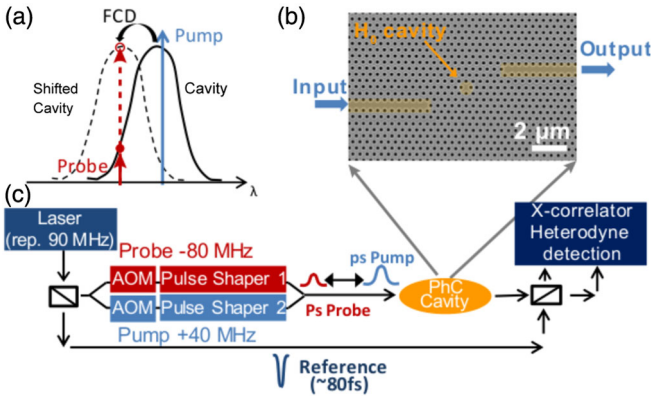

FIG. 1. (a) Principle of operation of a PhC cavity all-optical switch. (b) SEM image of the H_0 cavity and its access waveguides. (c) Schematic of the experiment. The picosecond pump and probe are carved from the same 80 fs reference pulse. Heterodyne detection using short reference pulses allows characterizing pulses with energy as low as 40 aJ/pulse and achieving 150 fs deconvolution-free temporal resolution.

been considered. In particular, the coherent interaction of the pump and probe, namely, wave mixing, has to the best of our knowledge been neglected so far in all models and interpretations of TPA-based switching dynamics, although it is well known that it plays an important role on the dynamics of quantum dot–PhC cavity systems [28] and active semiconductor waveguides on short time scales [29]. A good understanding of the different mechanisms governing the ultrafast switching of a semiconductor microcavity is indeed essential for the optimization of future all-optical switches.

In this work, we utilize a pump-probe technique based on a heterodyne detection scheme [30] that allows measuring the temporal trace of weak probe pulses spectrally overlapping with a pump pulse, with a temporal and energetic resolution of ≤ 100 fs and ≤ 40 aJ/pulse, respectively. Compared to other techniques for characterizing the response of similar photonic devices [31], the use of acousto-optic modulators to "label" the different pulses in the heterodyne detection allows investigating structures suited for integrated photonic chips, where the pump and probe copropagate through the same channels. Notice that the rf labeling employed by the heterodyne technique is very well suited to characterize coherent four-wave interactions between the pump and probe and, in particular, to distinguish these effects from incoherent processes (e.g., cross-phase modulation and frequency shift).

We investigate the switching dynamics in the ultrafast regime and show, in particular, that the fast modulation of the cavity gives rise to a large parametric gain (>10 dB) induced by population oscillations of the free-carrier plasma. This coherent process adds to the classical switching mechanism that is observed for long time scales. By generalizing the classical temporally coupled mode theory used so far to describe switching dynamics [22,32,33] to include coherent pump-probe interactions, very good agreement between the experiment and theory is obtained (see Supplemental Material [34]).

We consider a photonic crystal InP membrane with an H_0 nanocavity [35] coupled with access waveguides as seen in Fig. 1(b). InP exhibits TPA at the excitation wavelength of 1.55 μm (the gap is 1.34 eV [36]). The quality factor of the cavities that we studied is on the order $Q = 1000$–3000, corresponding to a cavity lifetime of 0.8–2.5 ps, thus being on the same order as the fast diffusion time (about 3 ps [5]) of the free carriers. The relevant experimental parameters are presented in Table I. Note that cavities with an ultrahigh quality factor, working at lower speed, can experience also other phenomena like, for example, regenerative oscillations [37–39] or self-pulsing [40], but they happen on a much longer time scale than the effects investigated here.

In previous experiments [5,32], only the total (integrated) probe output energy was detected. Here, we retrieved the temporal shape of the transmitted probe. Using pulse shapers, we shaped Gaussian picosecond pump and probe pulses to be Fourier limited at the input of the waveguide and matching the PhC cavity spectral width. The reference, propagating entirely in free space, was close to Fourier limited with a duration of 0.1 ps. Typically, the time-averaged signal from the balanced detector in heterodyne cross-correlation measurements is a function of the probe-reference delay, which can be written as a convolution of the two pulse envelopes times a sine function oscillating at the frequency induced by the AOM [29,41]. Considering the short duration of the reference pulse, scanning the reference-probe delay stage is nearly equivalent to recording the probe envelope without the convolution issues that usually smear the temporal features in cross-correlation measurements [33].

TABLE I. Experimentally measured parameters. τ, Q, δ, and U refer to the pulse FWHM duration, cavity quality factor, frequency detuning relative to the cold cavity resonance, and estimated pulse energy coupled into the waveguide, respectively. Subindices pr, p, and r refer to the probe, pump, and reference, respectively.

Parameter	Value	Parameter	Value
λ_0	1548 nm	Q	966
τ_p	0.70 ps	τ_{pr}	2.2 ps
U_p	80 fJ	U_{pr}	1.5 fJ
$\delta_p = \delta_{pr} = \delta_i$	0.0 ps^{-1}	τ_r	0.1 ps

We consider the PhC cavity switch in a switch-off configuration, where the probe and pump are set on resonance with the unperturbed "cold" cavity. As the cavity shifts under the action of the pump, the probe transmission drops. For each pump-probe delay, we retrieved the transmitted probe envelope simply by scanning the reference stage. Differential transmission is obtained by recording the probe trace both with and without the pump present. The resulting transmission map is presented in Fig. 2(a).

For large negative pump-probe delays, the probe arrives well before the pump. Its shape is nearly symmetric, indicating a good match between the probe duration and the cavity response. Moreover, its transmission is not perturbed by the pump. For positive pump-probe delays, the probe is first suppressed and subsequently recovers within ~10 ps due to a combination of carrier diffusion and nonradiative recombination [5]. This is associated with a blueshift of the cavity resonance caused by the presence of the free carriers, leading to a reduction of the probe transmission and followed by relaxation back towards equilibrium [5,33]. For an overlapping pump and probe (pump-probe delay of ~0 ps), the dynamic blueshift of the resonance causes an adiabatic frequency shift of the probe [27]. This was directly observable from the measured phase change which shows a chirping across the probe envelope of 2.5 ps^{-1} corresponding to an about 3 nm frequency shift.

However, for negative pump-probe delays, where the pump pulse excites the cavity just after the probe has entered, a strong and unexpected *increase* in the transmission of the probe signal is observed corresponding to a

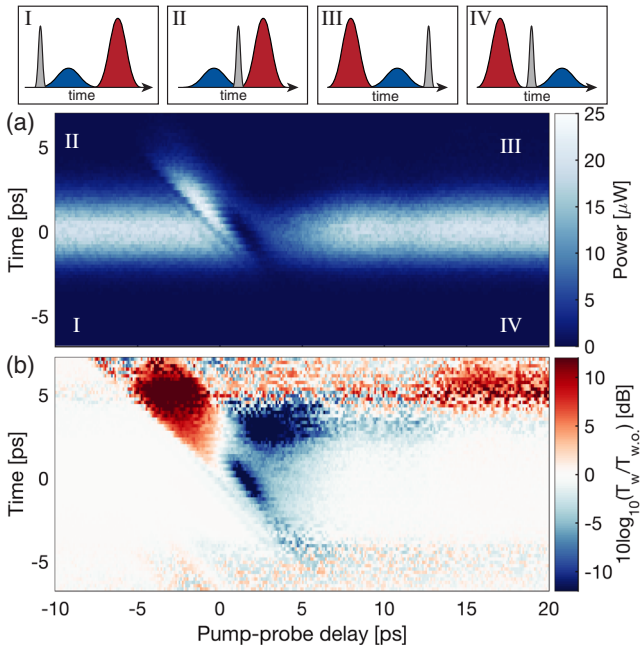

FIG. 2. Switch-off dynamics. (a) Measured probe trace as a function of the pump-probe delay. Y axis ("Time") corresponds to the reference-probe delay: The ultrashort duration of the reference pulse implies near-instantaneous gating. The temporal sequences of the reference (gray), pump (red), and probe (blue) pulses at points I–IV are illustrated. (b) Measured differential probe transmission in decibels (transmission with the pump on divided by transmission with the pump off). Pump and probe pulses are set on resonance with the cold cavity and have temporal widths of about 1 and 2 ps, respectively.

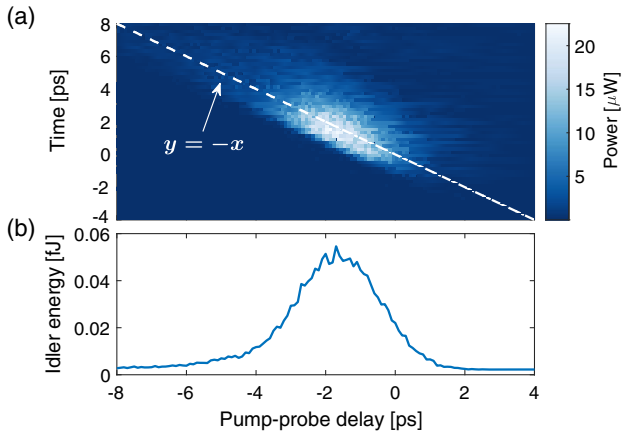

FIG. 3. (a) Measured envelope of the idler pulse, obtained by monitoring the signal at the beating frequency associated with the idler, as a function of the pump-probe delay and reference delay. Dashed line indicates a coincidence of the pump and reference pulse peaks. (b) Total idler energy versus pump-probe delay.

secondary peak. This effect has to our knowledge not been observed before. Previous models developed for long pulses and neglecting coherent mixing effects account only for a reduction in transmission.

The significance of the effect is particularly well illustrated in Fig. 2(b), showing the transmission ratio of the probe with and without the pump. Here, blue (red) areas indicate transmission suppression (enhancement). For pump delays of ~ -3 ps, the transient transmission is increased by more than 10 dB.

We ascribe the transient increase of the probe transmission to parametric gain caused by four-wave mixing that amplifies the tail of the probe pulse as soon as the pump starts entering the cavity. This interpretation is tested by investigating the presence of an associated idler signal at the same temporal position as the secondary peak is observed. The heterodyne detection technique used in our experiments is practical in this aspect, since the idler signal can be selected by filtering at the proper rf beating frequency [29].

The signal at the idler frequency, presented in Fig. 3, has indeed a similar shape as the secondary peak in Fig. 2(a) and furthermore coincides with the pump arrival time (thick dashed white line). The total idler energy is plotted in Fig. 2(b). We also recorded in Fig. 4(a) the idler's temporal envelope for a fixed pump-probe delay of -2 ps and varying pump pulse energies. We also show theoretical results [Fig. 4(b)] obtained by generalizing the coupled-mode theory [5,22,33] to include coherent wave mixing.

As the pump energy is increased, the envelope gradually shifts towards earlier times. The corresponding total idler energy relative to the input probe energy is shown in Fig. 4(c). The experimental measurements have been scaled to correspond with the theoretical values for the lowest energy. The energy of the idler pulse quickly increases with the pump energy and saturates for pump energies above 100–150 fJ. For the lowest pump powers, the idler energy clearly scales with the pump power to the power of 3, as indicated with the dashed line. Such a scaling differs from the square scaling that is expected for Kerr ($\chi^{(3)}$)-based parametric amplification [42,43].

As the pump enters the cavity, the induced resonance shift affects both the phase matching between the pump, probe, and idler as well as the coupling of the probe into and out of the cavity. As a result, for a moderate pump energy, all three waves remain on resonance within the cavity, and the parametric process builds up and results in a large output idler energy [44].

For a large pump energy, the front of the pump pulse shifts the resonance to such an extent that the remaining tail of the pump is prohibited from coupling into the cavity. The higher intrinsic gain due to a higher pump power is thus compensated by a decreased interaction time [45]. This also results in a decrease of the idler pulse arrival time for an increasing pump power. Differences between the theory and experiment appear for the highest pump energies and are attributed the limitations of the model, where, e.g., thermal effects are not included. In case the probe is initially blue-detuned with respect to the cavity, the device acts in a switching-on configuration, and the

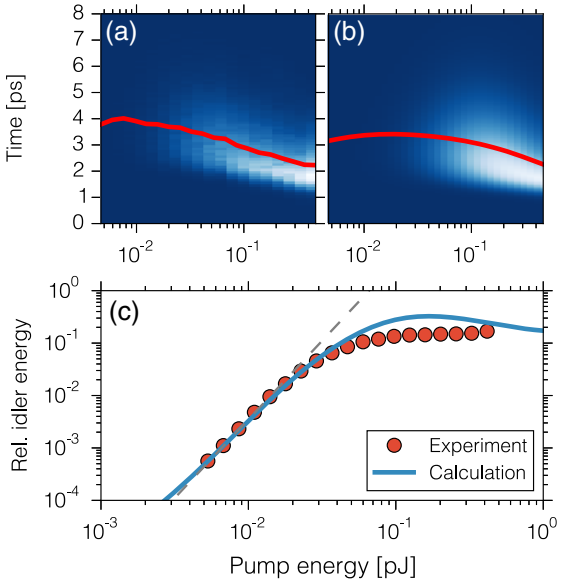

FIG. 4. (a) Measured envelope of the idler pulse as a function of the coupled pump pulse energy and reference delay (Time). The pump-probe delay was set at −2 ps. Red line indicates the temporal mean (first moment). (b) Corresponding theoretical results. (c) Idler energy relative to the input probe pulse energy, obtained by integration of results depicted in (a) and (b) along the time axis. Red circle markers indicate experimental data, and the solid blue line presents the calculated result. The dashed line is a guide to the eye indicating a third-order power scaling ($y = ax^3$).

transmission enhancement due to parametric gain as well as the classical cavity frequency shift add up. In particular, the double-peak feature as seen in Fig. 5 is merged into one single large output signal pulse. This renders the gain feature less visible on the signal.

In order to estimate the gain level, we performed additional measurements on another sample where we recorded both the idler and the probe trace. The results are presented in Fig. 5. Data presented in this figure would correspond to a vertical cut (Y axis) performed on both Figs. 2(a) and 3(a) and provides a better view of the exact temporal dynamics of the probe or idler.

The secondary peak is seen to coincide with the temporal position of the idler. In addition, the total gain is here as high as 8 dB, and the amplified probe even exceeds by 2 dB the maximal reference probe amplitude at $t = 0$ ps when the pump is turned off. Moreover, the total probe energy has been increased by about 3 dB, which could not be obtained by pulse reshaping, further confirming that the secondary peak is a parametric-gain effect. This degree of amplification is remarkable, considering that previous four-wave mixing experiments on Si PhC waveguides [43] demonstrated a maximum of −14 dB probe-idler conversion, despite the fact that the active device in Ref. [43] is more than 100 times longer than our cavity.

Finally, we investigated the origin of the parametric gain by comparing in Fig. 6 experimental data with numerical

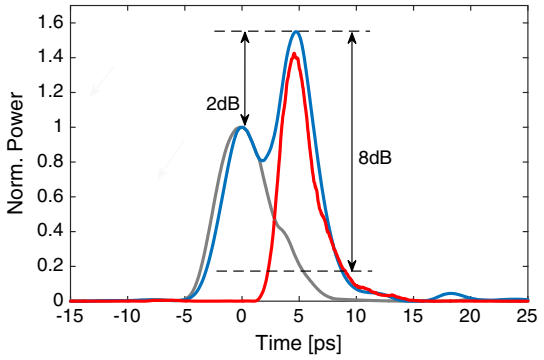

FIG. 5. Measured temporal traces of the idler (red), as well as the probe with (blue) and without (gray) the presence of the pump. The pump power is about 120 fJ/pulse, and the pump-probe delay is set to −3 ps.

models taking into account coherent pump-probe mixing. It is clear that FCD is responsible for the parametric gain, while the Kerr effect has little influence on the overall dynamics. Thus, the interference between the probe and the pump leads to a temporal modulation of the free-carrier generation rate. In turn, the coherent oscillation of the free-carrier population modulates the refractive index of the cavity via FCD, that scatters the strong pump into the probe and idler. The bandwidth of the parametric gain (i.e., the admissible pump-probe detuning) is directly related to the lifetime of the free-carrier population, since the corresponding bandwidth must sustain the pump-probe beat frequency. Thus, both fast diffusion and slower carrier recombination [5] may be important, depending on the pump-probe-cavity detuning. A shorter free-carrier relaxation time thus supports a parametric gain at higher detunings (beat frequencies).

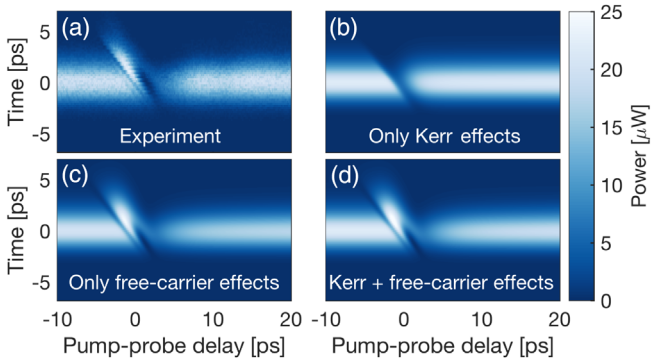

FIG. 6. (a) Color map of the probe temporal trace for various pump-probe delays. The pump power is about 130 fJ/pulse. (a) Experimental map. (b) Simulation wherein the FCD due to the fast free-carrier plasma is neglected. (c) Simulation wherein the Kerr effect is turned off. (d) Full model simulation including both FCD and Kerr effects. When no nonlinear effects are present, the probe is a trace that looks like the one seen at large negative pump-probe delay in (a)–(d).

In conclusion, we have presented temporally resolved pump-probe transmission measurements of an ultrafast PhC all-optical switch, showing the appearance of strong coherent effects. In particular, four-wave mixing induced by oscillations of the spatially localized free carriers in the nanocavity leads to more than 10 dB parametric gain of the probe and the generation of a strong idler signal. Such wave mixing, induced by population oscillations, is already known in semiconductor optical amplifiers that are several hundred micrometers long [46,47]. Here, however, the interaction takes place in a cavity with an extent that is a fraction of a wavelength and relies on cavity-enhanced two-photon absorption rather than normal linear absorption. Further understanding the role of such coherent dynamics is expected to be important for the development of photonic switches, possibly offering new regimes of ultrafast switching based on coherent effects.

This work was supported by the Villum Foundation through the VKR center of excellence NAnophotonics for TErabit Communications (NATEC, Grant No. 8692) and the Danish Research Council for Independent Research (Grant No. FTP 11-116740). The authors thank M. Heuck for fruitful discussions and K. Yvind for assistance on device fabrication.

P. C. and P. L. contributed equally to this work.

*jesm@fotonik.dtu.dk

[1] D. A. B. Miller, Proc. IEEE **97**, 1166 (2009).
[2] T. Tanabe, M. Notomi, S. Mitsugi, A. Shinya, and E. Kuramochi, Appl. Phys. Lett. **87**, 151112 (2005).
[3] A. Shinya, S. Matsuo, Yosia, T. Tanabe, E. Kuramochi, T. Sato, T. Kakitsuka, and M. Notomi, Opt. Express **16**, 19382 (2008).
[4] C. Husko, A. D. Rossi, S. Combrié, Q. Tranh, F. Raineri, and C. Wong, Appl. Phys. Lett. **94**, 021111 (2009).
[5] Y. Yu, E. Palushani, M. Heuck, N. Kuznetsova, P. T. Kristensen, S. E. D. Vukovic, C. Peucheret, L. K. Oxenløwe, S. Combri'e, A. de Rossi, K. Yvind, and J. Mørk, Opt. Express **21**, 31047 (2013).
[6] D. Vukovic, Y. Yu, M. Heuck, S. Ek, N. Kuznetsova, P. Colman, E. Palushani, J. Xu, K. Yvind, L. Oxenløwe, J. Mørk, and C. Peucheret, IEEE Photonics Technol. Lett. **26**, 257 (2014).
[7] K. Nozaki, T. Tanabe, A. Shinya, S. Matsuo, T. Sato, H. Taniyama, and M. Notomi, Nat. Photonics **4**, 477 (2010).
[8] T. Tanabe, M. Notomi, S. Mitsugi, A. Shinya, and E. Kuramochi, Opt. Lett. **30**, 2575 (2005).
[9] M. Notomi, A. Shinya, S. Mitsugi, G. Kira, E. Kuramochi, and T. Tanabe, Opt. Express **13**, 2678 (2005).
[10] S. Lan, A. V. Gopal, K. Kanamoto, and H. Ishikawa, Appl. Phys. Lett. **84**, 5124 (2004).
[11] I. Fushman, E. Waks, D. Englund, N. Stoltz, P. Petroff, and J. Vukovic, Appl. Phys. Lett. **90**, 091118 (2007).
[12] S. Matsuo, A. Shinya, T. Kakitsuka, K. Nozaki, T. Segawa, T. Sato, Y. Kawaguchi, and M. Notomi, Nat. Photonics **4**, 648 (2010).
[13] B. R. Bennett, R. A. Soref, and J. A. Del Alamo, IEEE J. Quantum Electron. **26**, 113 (1990).
[14] D. Englund, A. Majumdar, M. Bajcsy, A. Faraon, P. Petroff, and J. Vuckovic, Phys. Rev. Lett. **108**, 093604 (2012).
[15] R. Bose, D. Sridharan, H. Kim, G. Solomon, and E. Waks, Phys. Rev. Lett. **108**, 227402 (2012).
[16] G. Moille, S. Combrié, L. Morgenroth, G. Lehoucq, F. Neuilly, B. Hu, D. Decoster, and A. de Rossi, Laser Photonics Rev. **10**, 409 (2016).
[17] J. Bravo-Abad, A. Rodriguez, P. Bermel, S. G. Johnson, J. D. Joannopoulos, and M. Soljacic, Opt. Express **15**, 16161 (2007).
[18] S. Fan, Appl. Phys. Lett. **80**, 908 (2002).
[19] X. Yang, C. Husco, C. W. Wong, M. Yu, and D. L. Kwong, Appl. Phys. Lett. **91**, 051113 (2007).
[20] Y. Yu, Y. Chen, H. Hu, W. Xue, K. Yvind, and J. Mørk, Laser Photonics Rev. **9**, 241 (2015).
[21] Y. Yu, H. Hu, L. K. Oxenløwe, K. Yvind, and J. Mørk, Opt. Lett. **40**, 2357 (2015).
[22] A. de Rossi, M. Lauritano, S. Combrié, Q. V. Tran, and C. Husko, Phys. Rev. A **79**, 043818 (2009).
[23] E. Weidner, S. Combrié, A. de Rossi, Q. N. V. Tran, and S. Cassette, Appl. Phys. Lett. **90**, 101118 (2007).
[24] M. Notomi and S. Mitsugi, Phys. Rev. A **73**, 051803(R) (2006).
[25] S. F. Preble, Q. Xu, and M. Lipson, Nat. Photonics **1**, 293 (2007).
[26] P. J. Harding, H. J. Bakker, A. Hartsuiker, J. Claudon, A. P. Mosk, J.-M. Gérard, and W. L. Vos, J. Opt. Soc. Am. B **29**, A1 (2012).
[27] T. Kampfrath, D. M. Beggs, T. P. White, A. Melloni, T. F. Krauss, and L. Kuipers, Phys. Rev. A **81**, 043837 (2010).
[28] R. Bose, T. Cai, K. Choudhury, G. Solomon, and E. Waks, Nat. Photonics **8**, 858 (2014).
[29] A. Mecozzi and J. Mørk, J. Opt. Soc. Am. B **13**, 2437 (1996).
[30] K. L. Hall, G. Lenz, E. P. Ippen, and G. Raybon, Opt. Lett. **17**, 874 (1992).
[31] T. Kampfrath, D. M. Beggs, T. F. Krauss, and L. K. Kuipers, Opt. Lett. **34**, 3418 (2009).
[32] Y. Yu, E. Palushani, M. Heuck, D. Vukovic, C. Peucheret, K. Yvind, and J. Mørk, Appl. Phys. Lett. **105**, 071112 (2014).
[33] M. Heuck, S. Combrié, G. Lehoucq, S. Malaguti, G. Bellanca, S. Trillo, P. T. Kristensen, J. Mørk, J. P. Reithmaier, and A. de Rossi, Appl. Phys. Lett. **103**, 181120 (2013).
[34] See Supplemental Material at http://link.aps.org/supplemental/10.1103/PhysRevLett.117.233901 for further information on the experimental set-up, the sample and the theoretical model.
[35] K. Nozaki and T. Baba, Appl. Phys. Lett. **88**, 211101 (2006).
[36] D. R. Lide, *Handbook of Chemistry and Physics*, 87th ed. (CRC Press, Boca Raton, FL, 1998).
[37] N. Cazier, X. Checoury, L.-D. Haret, and P. Boucaud, Opt. Express **21**, 13626 (2013).
[38] J. Yang, T. Gu, J. Zheng, M. Yu, G.-Q. Lo, D.-L. Kwong, and C. Wei Wong, Appl. Phys. Lett. **104**, 061104 (2014).
[39] T. Gu, N. Petrone, J. F. McMillan, A. van der Zande, M. Yu, G. Q. Lo, D. L. K. Wong, J. Hone, and C. W. Wong, Nat. Photonics **6**, 554 (2012).

[40] V. Grigoriev and F. Biancalana, Phys. Rev. A **83**, 043816 (2011).
[41] H. Gersen, J. P. Korterik, N. F. van Hulst, and L. Kuipers, Phys. Rev. E **68**, 026604 (2003).
[42] J. Li, L. O'Faolain, I. H. Rey, and T. F. Krauss, Opt. Express **19**, 4458 (2011).
[43] C. Monat, M. Ebnali-Heidari, C. Grillet, B. Corcoran, B. J. Eggleton, T. P. White, L. O'Faolain, J. Li, and T. F. Krauss, Opt. Express **18**, 22915 (2010).
[44] A. Martin, G. Moille, S. Combrié, G. Lehoucq, T. Debuisschert, J. Lian, S. Sokolov, A. P. Mosk, and A. de Rossi, arXiv:1602.04833.
[45] P. Colman, I. Cestier, A. Willinger, S. Combrié, G. Lehoucq, G. Eisenstein, and A. D. Rossi, Opt. Lett. **36**, 2629 (2011).
[46] A. Uskov, J. Mork, and J. Mark, IEEE J. Quantum Electron. **30**, 1769 (1994).
[47] J. Mørk and A. Mecozzi, IEEE J. Quantum Electron. **33**, 545 (1997).